Structuring Time in Human Lateral Entorhinal Cortex

Jacob L.S. Bellmund[1,2,3*], Lorena Deuker[4], Christian F. Doeller[1,2*]

1: Max Planck Institute for Human Cognitive and Brain Sciences, Leipzig, Germany
2: Kavli Institute for Systems Neuroscience, Centre for Neural Computation, The Egil and Pauline Braathen and Fred Kavli Centre for Cortical Microcircuits, NTNU, Norwegian University of Science and Technology, Trondheim, Norway
3: Donders Institute for Brain, Cognition and Behaviour, Radboud University, Nijmegen, the Netherlands
4: Ruhr-University, Bochum, Germany
* Corresponding authors. Email: bellmund@cbs.mpg.de; doeller@cbs.mpg.de

Summary

Episodic memories consist of event information linked to spatio-temporal context. Notably, the hippocampus is involved in the encoding, representation and retrieval of temporal relations that comprise a context (Deuker et al., 2016; Tubridy and Davachi, 2011; DuBrow and Davachi, 2014; Ezzyat and Davachi, 2014; Hsieh et al., 2014; Jenkins and Ranganath, 2010, 2016; Kyle et al., 2015; Lositsky et al., 2016; Nielson et al., 2015; Copara et al., 2014), but it remains largely unclear how coding for elapsed time arises in the hippocampal-entorhinal region. The entorhinal cortex (EC), the main cortical input structure of the hippocampus, has been hypothesized to provide temporal tags for memories via contextual drift (Howard and Kahana, 2002; Howard et al., 2005). Recent evidence demonstrates that time can be decoded from population activity in the rodent lateral EC, putatively arising from the integration of experience (Tsao et al., 2018). Here, we asked how learning a temporal structure influences entorhinal event representations. Participants acquired knowledge about temporal and spatial relationships between object positions—dissociated via teleporters—along a fixed route through a virtual city. We analyze fMRI multi-voxel pattern similarity change from before to after learning in the EC. Object representations in the anterior-lateral EC (alEC) specifically, the human homologue of rodent lateral EC (Navarro Schröder et al., 2015; Maass et al., 2015), changed to reflect elapsed time between events. Holistic representations of the temporal structure in alEC related to memory recall behavior suggesting mental traversals of the route during retrieval. Furthermore, we reconstructed the temporal structure of object relationships from alEC pattern similarity change. Our findings demonstrate that the experienced temporal structure of events shapes representations in the alEC, potentially via the reactivation of temporal context representations derived from slowly-varying population signals during learning. This provides novel evidence for the role of the human lateral EC in representing time for episodic memory.

Results

Here, we used representational similarity analysis of fMRI multi-voxel patterns in the hippocampal-entorhinal region to test the prediction that the anterior-lateral entorhinal cortex (alEC) maps the temporal structure of events. We examined the effect of learning temporal and spatial positions of objects along a route through a virtual city (Figure 1). Specifically, we presented object images twelve times before and after learning, using the same random order in both scanning runs. We compared the change in neural pattern similarity between object representations to the temporal and spatial structure of the task (Deuker et al., 2016). Using this paradigm and data, we previously demonstrated that participants can successfully recall the subjective, remembered spatial and temporal relations between object pairs and that the change of hippocampal representations reflects an integrated event map of the remembered distance structure. Here, we demonstrate that the change of multi-voxel pattern similarity through learning in alEC (Figure 2A) reflects the objective temporal distance structure of the task—dissociated from spatial distances through the use of teleporters (Deuker et al., 2016)—

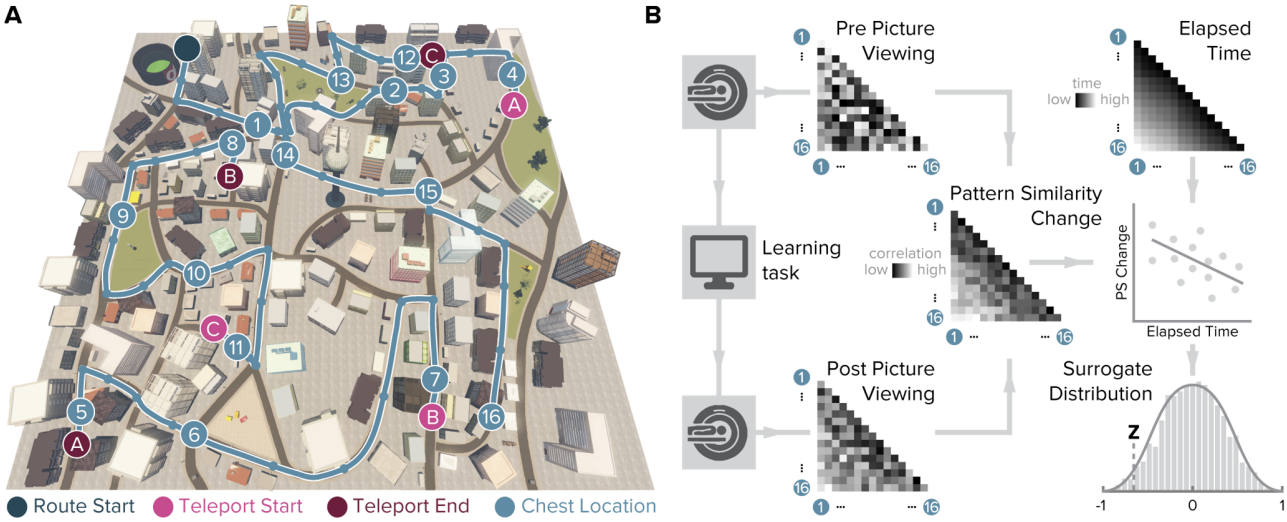

Figure 1. Design and analysis logic. A. During the spatio-temporal learning task, which took place in between two identical runs of a picture viewing task (Figure S1), participants repeatedly navigated a fixed route (blue line, mean ± standard deviation of median time per lap 264.6±47.8s) through the virtual city along which they encountered objects hidden in chests (numbered circles) (Deuker et al., 2016). Temporal (median time elapsed) and spatial (Euclidean) distances between objects were dissociated through the use of three teleporters (lettered circles) along the route (Figure S2), which instantaneously changed the participant's location to a different part of the city. **B.** In the picture viewing tasks, participants viewed randomly ordered images of the objects encountered along the route while fMRI data were acquired. We quantified multi-voxel pattern similarity change between pairwise object comparisons from before to after learning the temporal and spatial relationships between objects in subregions of the entorhinal cortex. We tested whether pattern similarity change reflected the structure of the task, by correlating it with the time elapsed between objects pairs (top right matrix shows median elapsed time between object encounters along the route averaged across participants). For each participant, we compared the correlation between pattern similarity change and the prediction matrix to a surrogate distribution obtained via bootstrapping and used the resulting z-statistic for group-level analysis (see Methods).

resulting in a consistent relationship between similarity and time elapsed between object encounters. The change in multi-voxel pattern similarity in alEC between pre- and post-learning scans was negatively correlated with temporal distances between objects pairs along the route (Figure 2B, T(25)=- 3.75, p=0.001, alpha-level of 0.0125, Bonferroni-corrected for four

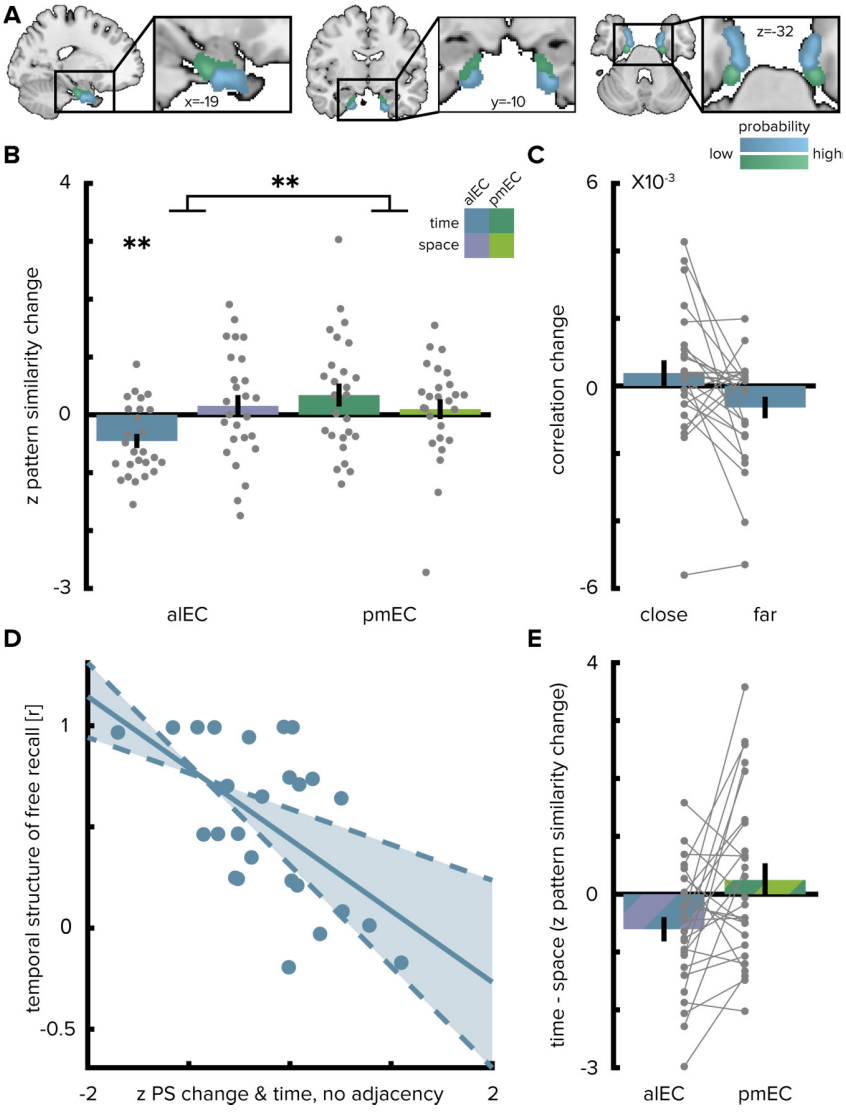

Figure 2. Temporal mapping in alEC. A. Entorhinal cortex subregion masks from (Navarro Schröder et al., 2015) were moved into subject-space and intersected with participant-specific Freesurfer parcellations of entorhinal cortex. Color indicates probability of voxels to belong to the alEC (blue) or pmEC (green) subregion mask after subject-specific masks were transformed back to MNI template space for visualization. **B.** Pattern similarity change in the alEC reflected elapsed time between objects along the route as indicated by z-statistics significantly below 0. A permutation-based two-way repeated measures ANOVA further revealed a significant interaction highlighting a difference in temporal and spatial mapping between alEC

and pmEC. **C.** Pattern similarity change in alEC for objects encountered close together or far apart in time along the route. **D.** Pattern similarity change in alEC was negatively related to temporal relationships above and beyond increased similarity for objects encountered in direct succession (Figure S3A). The magnitude of this effect correlated significantly with participants' free recall behavior. The temporal structure of freely recalled objects was assessed by calculating the absolute difference in position for all recalled objects and correlating this difference with the time elapsed between encounters of object pairs along the route. Solid line shows least squares line; dashed lines and shaded region highlight bootstrapped confidence intervals. PS: pattern similarity **E.** To illustrate the interaction effect shown in **B**, the difference in the relationship between temporal and spatial distances to pattern similarity change is shown for alEC and pmEC. Negative values indicate stronger correlations with temporal compared to spatial distances. Bars show mean and S.E.M with lines connecting data points from the same participant in **C** and **E**.

comparisons). Pattern similarity change in alEC also correlated negatively with ordinal distances between object pairs ($T(25)=-3.37$, $p=0.002$), closely related to elapsed time in our task (mean±standard deviation Pearson $r=0.993\pm0.0014$). Objects encountered in temporal proximity changed to be represented more similarly compared to object pairs further separated in time (Figure 2C).

To test whether this effect was not only due to increased similarity of objects encountered in direct succession along the route ($T(25)=2.45$, $p=0.018$), we correlated residual pattern similarity change, i.e. variance that could not be explained by this adjacency model, with the time elapsed between object encounters (see Methods). Pattern similarity change was still negatively correlated with elapsed time ($T(25)=-1.82$, $p=0.041$, one-sided test, Figure S3A), speaking for holistic representations of temporal relationships in the alEC. Importantly, the strength of this effect was strongly related to behavior in the post-scan free recall test, where participants retrieved the objects from memory. Specifically, participants with stronger correlations between residual pattern similarity change and elapsed time tended to recall objects together that were encountered in temporal proximity along the route (Pearson $r=-0.56$, $p=0.003$, CIs: -0.76, -0.25, Figure 2D).

Pattern similarity change in alEC did not correlate significantly with spatial distances ($T(25)=0.81$, $p=0.420$) and pattern similarity change in posterior-medial EC (pmEC) did not correlate with spatial ($T(25)=0.58$, $p=0.583$) or temporal ($T(25)=1.73$, $p=0.089$) distances. Temporal distances from the first picture viewing task were not related to alEC pattern similarity change (Figure S3B; $T(24)=-0.29$ $p=0.776$, one outlier excluded, see Methods) and correlations with elapsed time were significantly more negative ($T(24)=-1.76$ $p=0.045$; one-sided test); strengthening our interpretation that pattern similarity changes reflected relationships experienced in the virtual city. We did not observe an association of pattern similarity change in the lateral occipital cortex with elapsed time, which might be expected if the observed effect would be related to the reinstatement of objects nearby in time (Figure S3C; $T(25)=-1.40$ $p=0.184$).

Can we reconstruct the timeline of events from pattern similarity change in alEC? Here, we used multidimensional scaling to extract coordinates along one dimension from pattern similarity change averaged across participants (Figure 3A-D). The reconstructed temporal coordinates, transformed into the original value range using Procrustes analysis (Figure 3A), mirrored the

time points at which objects were encountered during the task (Figure 3B, Pearson correlation between reconstructed and true time points, r=0.56, p=0.023, bootstrapped 95% confidence interval: 0.21, 0.79). Further, we contrasted the fit of the coordinates from multidimensional scaling between the true and randomly shuffled timelines (Figure 3C). Specifically, we compared the deviance of the fit between the reconstructed and the true timeline, the Procrustes distance, to a surrogate distribution of Procrustes distances. This surrogate distribution was obtained by fitting the coordinates from multidimensional scaling to randomly shuffled timelines of events. The Procrustes distance from fitting to the true timeline was smaller than the 5th percentile of the surrogate distribution generated via 10000 random shuffles (Figure 3D, p=0.026). Taken together, these findings indicate that alEC representations change through learning to reflect the temporal structure of the acquired event memories and that we can recover the timeline of events from this representational change.

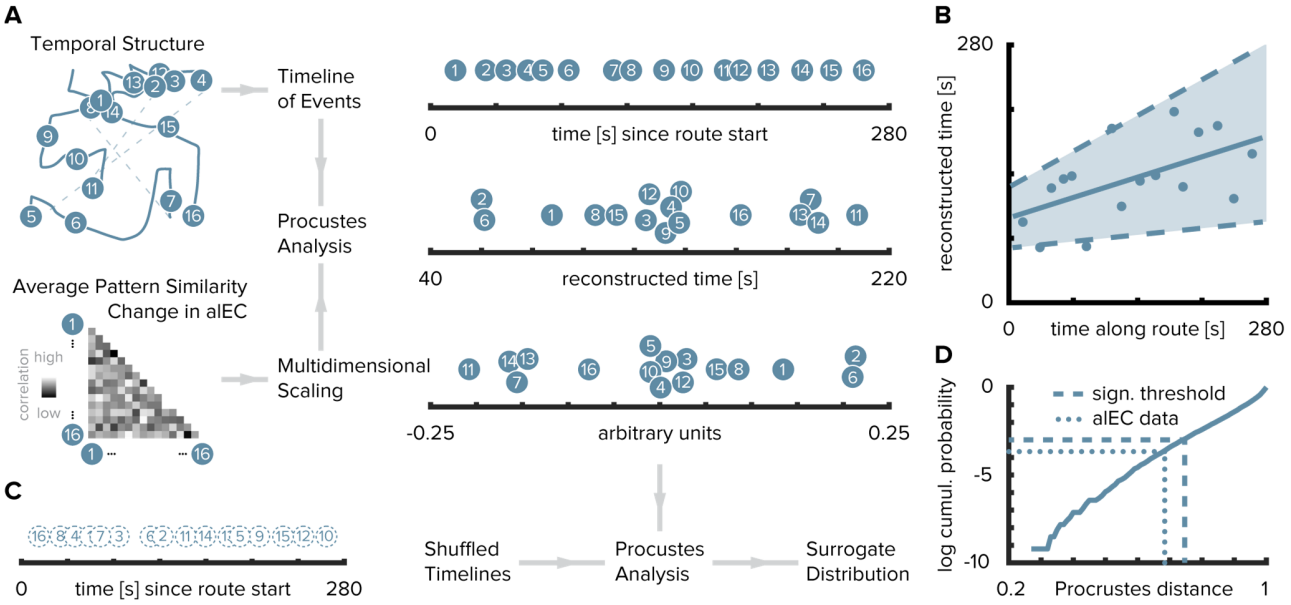

Figure 3. Timeline reconstruction. A. To recover the temporal structure of events we performed multidimensional scaling on the average pattern similarity change matrix in alEC. The resulting coordinates, one for each object along the route, were subjected to Procrustes analysis, which applies translations, rotations and uniform scaling to superimpose the coordinates from multidimensional scaling on the true temporal coordinates along the route (see Methods). For visualization, we varied the positions resulting from multidimensional scaling and Procrustes analysis along the y-axis. **B.** The temporal coordinates of this reconstructed timeline were significantly correlated with the true temporal coordinates of object encounters along the route. Circles indicate time points of object encounters; solid line shows least squares line; dashed lines and shaded region highlight bootstrapped confidence intervals. **C.** The goodness of fit of the reconstruction (the Procrustes distance) was compared to a surrogate distribution of Procrustes distances obtained from randomly shuffling the true coordinates against the coordinates obtained from multidimensional scaling and then performing Procrustes analysis for each of 10000 shuffles (left shows one randomly shuffled timeline for illustration). **D.** The Procrustes distance obtained from fitting to the true timeline of events (dotted line) was smaller than the 5th percentile (dashed line) of the surrogate distribution (solid line), which constitutes the significance threshold at an alpha level of 0.05.

What is the nature of regional specificity within entorhinal cortex? In a next step, we compared temporal and spatial mapping between the subregions of the entorhinal cortex (EC). We conducted a permutation-based two-by-two repeated measures ANOVA (see Methods) with the factors entorhinal subregion (alEC vs. pmEC) and relationship type (time elapsed vs. spatial distance between events). Crucially, we observed a sign ificant interaction between EC subregion and distance type ($F(1,25)=7.40$, $p=0.011$, Figure 2B and 2E). Further, the main effect of EC subregion was significant ($F(1,25)=5.18$, $p=0.029$), while the main effect of distance type was not ($F(1,25)=0.84$, $p=0.367$). Based on the significant interaction, we conducted planned post-hoc comparisons, which revealed significant differences (Bonferroni-corrected alpha-level of 0.025) between the mapping of elapsed time and spatial distance in alEC ($T(25)=-2.91$, $p=0.007$) and a significant difference between temporal mapping in alEC compared to pmEC ($T(25)=-3.52$, $p=0.001$). Spatial and temporal signal-to-noise ratios did not differ between alEC and pmEC (Figure S4), ruling out that differences in signal quality might explain the observed effects. Collectively, these findings demonstrate that, within the EC, only representations in the anterior-lateral subregion change to resemble the temporal structure of events and that this mapping was specific to the temporal rather than the spatial dimension.

Discussion

We examined the similarity of multi-voxel patterns to demonstrate that alEC event representations reflect experienced temporal relationships. Despite being cued in random order after learning, these representations related to a holistic temporal map of the task structure. Moreover, entorhinal pattern similarity related to participants' recall behavior and we recovered the timeline of events during learning from these representations.

Our hypothesis for temporal mapping in the alEC was based on a recent finding demonstrating that population activity in the rodent lateral EC carries information from which time can be decoded at different scales ranging from seconds to days (Tsao et al., 2018). Time could be decoded with higher accuracies from the lateral EC than the medial EC and hippocampal subfield CA3. This temporal information might arise from the integration of experience across different scales. During a structured task in which the animal ran repeated laps on a maze separated into different trials, neural trajectories through population activity space were similar across trials, illustrating that the dynamics of lateral EC neural signals were more stable than during free foraging (Tsao et al., 2018). Consistently, temporal coding was improved for time within a trial during the structured task compared to episodes of free foraging. These findings support the notion that temporal information in the lateral EC might inherently arise from the encoding of experience (Tsao et al., 2018). In our task, relevant factors contributing to a similar experience of the route on each lap are not only the encounters of objects in a specific order at their respective positions, but also recognizing and passing salient landmarks as well as navigational demands in general. Changes in metabolic states and arousal presumably varied more linearly over time. The long time scales of lateral EC temporal codes differ from the observation of time cells in the hippocampus and medial EC, which fire during temporal delays in highly trained tasks (Eichenbaum, 2014; Heys and Dombeck, 2018; Kraus et al., 2015;

MacDonald et al., 2011; Mau et al., 2018; Pastalkova et al., 2008). Time cell ensembles change over minutes and days (Mau et al., 2018), but their firing has been investigated in the context of short delays in the range of seconds. This leaves open the questions whether and how time cell sequences encode longer temporal intervals as in our task, where one lap of the route took approximately five minutes. Slowly drifting activity patterns have been observed also in the human medial temporal lobe (Folkerts et al., 2018) and EC specifically (Lositsky et al., 2016). A representation of time within a known trajectory in the aIEC could underlie the encoding of temporal relationships between events in our task, where participants repeatedly navigated along the route to learn the positions of objects. Hence, temporal mapping in the aIEC as we report here might help integrate hippocampal spatio-temporal event maps (Deuker et al., 2016).

One possibility for why the similarity structure of aIEC multi-voxel patterns resembles a holistic temporal map of the event memories after learning is the reactivation of temporal context information. If aIEC neural populations traverse similar population state trajectories on each lap, they would carry information about time within a lap. A given object would be associated with a similar aIEC population state on each lap. Associations with temporally drifting signals during the learning task would result in representational changes relative to the baseline scan that, if reactivated in the post-learning picture viewing task, reflect experienced temporal distances between objects and their order. This might explain the observed pattern similarity structure with relatively increased similarity for objects encountered in temporal proximity during learning and decreased similarity for items encountered after longer delays. While this interpretation is in line with data from rodent electrophysiology (Tsao et al., 2018) and the framework proposed by the temporal context model (Howard and Kahana, 2002; Howard et al., 2005), we cannot test the reinstatement of specific activity patterns from the learning phase directly since fMRI data were only collected during the picture viewing tasks in this study. The reactivation of temporal context representations might explain why the change in multi-voxel patterns in the aIEC reflects the temporal relations between objects representations after learning.

Importantly, the highly-controlled design of our study supports the interpretation that aIEC representations change through learning to map time elapsed between events. The order of object presentations during the scanning sessions was randomized and thus did not reflect the order in which objects were encountered during the learning task. Since the assignment of objects to positions was randomized across participants and we analyzed pattern similarity *change* from a baseline scan, our findings do not go back to prior associations between the objects, but reflect information learned over the course of the experiment. Further, we presented the object images during the scanning sessions not only in the same random order, but also with the same presentation times and inter-stimulus intervals; thereby ruling out that the effects we observed go back to temporal autocorrelation of the BOLD-signal. Taken together, the high degree of experimental control of our study supports the conclusion that aIEC representations change to reflect the temporal structure of acquired memories.

Our assessment of temporal representations in the antero-lateral and posterior-medial subdivision of the EC was inspired by a recent report of temporal coding during free foraging and repetitive behavior in the rodent EC, which was most pronounced in the lateral EC (Tsao et al., 2018). In humans, local and global functional connectivity patterns suggest a preserved

bipartite division of the EC, but along not only its medial-lateral, but also its anterior-posterior axis (Navarro Schröder et al., 2015; Maass et al., 2015). Via these entorhinal subdivisions, cortical inputs from the anterior-temporal and posterior-medial memory systems might converge onto the hippocampus (Ranganath and Ritchey, 2012; Ritchey et al., 2015).

Our findings are in line with the role of the hippocampus in the retrieval of temporal information from memory (Copara et al., 2014; DuBrow and Davachi, 2014; Kyle et al., 2015; Nielson et al., 2015). Hippocampal pattern similarity has been shown to scale with temporal distances between events (Deuker et al., 2016; Nielson et al., 2015) and evidence for the reinstatement of temporally associated items from memory has been reported in the hippocampus (DuBrow and Davachi, 2014). Already at the stage of encoding, hippocampal and entorhinal activity have been related to later temporal memory (DuBrow and Davachi, 2014, 2016; Ezzyat and Davachi, 2014; Jenkins and Ranganath, 2010, 2016; Lositsky et al., 2016; Tubridy and Davachi, 2011). For example, increased pattern similarity has been reported for items remembered to be close together compared to items remembered to be far apart in time, despite the same time having elapsed between these items (Ezzyat and Davachi, 2014). Similarly, changes in EC pattern similarity during the encoding of a narrative correlated with later duration estimates between events (Lositsky et al., 2016). Complementing these reports, our findings demonstrate that entorhinal activity patterns carry information about the temporal structure of memories at retrieval. Furthermore, the degree to which EC patterns reflected holistic representations of temporal relationships related to recall behavior characterized by the consecutive reproduction of objects encountered in temporal proximity; potentially through mental traversals of the route during memory recall. The central role of the hippocampus and entorhinal cortex in temporal memory (for review see (Davachi and DuBrow, 2015; Howard, 2018; Ranganath, 2018; Wang and Diana, 2017)) dovetails with the involvement of these regions in learning sequences and statistical regularities in general (Barnett et al., 2014; Garvert et al., 2017; Hsieh et al., 2014; Kumaran and Maguire, 2006; Schapiro et al., 2012, 2016; Thavabalasingam et al., 2018)).

In conclusion, our findings demonstrate that activity patterns in alEC, the human homologue region of the rodent lateral EC, carry information about the temporal structure of newly acquired memories. The observed effects might be related to the reactivation of temporal contextual tags, in line with the recent report of temporal information available in rodent lateral EC population activity and models of episodic memory.

Methods

Subjects

26 participants (mean±std. 24.88±2.21 years of age, 42.3% female) were recruited via the university's online recruitment system and participated in the study. As described in the original publication using this dataset (Deuker et al., 2016), this sample size was based on a power-calculation (alpha-level of 0.001, power of 0.95, estimated effect size of d=1.03 based on a prior study (Milivojevic et al., 2015)) using G*Power (http://www.gpower.hhu.de/). Participants with prior knowledge of the virtual city (see (Deuker et al., 2016)) were recruited for the study. All procedures were approved by the local ethics committee (CMO Regio Arnhem Nijmegen) and all participants gave written informed consent prior to commencement of the study.

Design

Overview

The experiment began by a 10 minute session during which participants freely navigated the virtual city (Bellmund et al., 2018) on a computer screen to re-familiarize themselves with its layout. Afterwards participants were moved into the scanner and completed the first run of the picture viewing task during which they viewed pictures of everyday objects as described below (Figure S1). After this baseline scan, participants learned a fixed route through the virtual city along which they encountered the objects at predefined positions (Figure 1 and Figure S1). The use of teleporters, which instantaneously moved participants to a different part of the city, enabled us to dissociate temporal and spatial distances between object positions (Figure S2). Subsequent to the spatio-temporal learning task, participants again underwent fMRI and completed the second run of the picture viewing task. Lastly, participants' memory was probed outside of the MRI scanner. Specifically, participants freely recalled the objects they encountered, estimated spatial and temporal distances between them on a subjective scale, and indicated their knowledge of the positions the objects in the virtual city on a top-down map (Deuker et al., 2016).

Spatio-temporal learning task

Participants learned the positions of everyday objects along a trajectory through the virtual city Donderstown (Bellmund et al., 2018). This urban environment, surrounded by a range of mountains, consists of a complex street network, parks and buildings. Participants with prior knowledge of the virtual city (see (Deuker et al., 2016)) were recruited for the study. After the baseline scan, participants navigated the fixed route through the city along which they encountered 16 wooden chests at specified positions (Figure 1A). During the initial 6 laps the route was marked by traffic cones. In later laps, participants had to rely on their memory to navigate the route, but guidance in the form of traffic cones was available upon button press for laps 7-11. Participants completed 14 laps of the route in total (mean ± standard deviation of duration 71.63±13.75 minutes), which were separated by a black screen displayed for 15s before commencement of the next lap from the start position.

Participants were instructed to open the chests they encountered along the route by walking into them. They were then shown the object contained in that chest for 2 seconds on a black screen. A given chest always contained the same object for a participant, with the assignment of objects to chests randomized across participants. Therefore, each object was associated with a spatial position defined by its location in the virtual city and a temporal position described by its occurrence along the progression of the route. Importantly, we dissociated temporal relationships between object pairs (measured by time elapsed between their encounter) from the Euclidean distance between their positions in the city through the use of teleporters. Specifically, at three locations along the route participants encountered teleporters, which immediately transported them to a different position in the city where the route continued (Figure 1A). This manipulation allows the otherwise impossible encounter of objects after only a short temporal delay, but with a large Euclidean distance between them in the virtual city (Deuker et al., 2016). Indeed, temporal and spatial distances across all comparisons of object pairs were uncorrelated (Pearson r=-0.068; bootstrapped 95% confidence interval: -0.24, 0.12; p=0.462; Figure S2).

Picture viewing tasks

Before and after the spatio-temporal learning task participants completed the picture viewing tasks while undergoing fMRI (Deuker et al., 2016). During these picture viewing tasks, the 16 objects from the learning task as well as an additional target object were presented. Participants were instructed to attend to the objects and to respond via button press when the target object was presented. Every object was shown 12 times in 12 blocks, with every object being shown once in every block. In each block, the order of objects was randomized. Blocks were separated by a 30 second break without object presentation. Objects were presented for 2.5 seconds on a black background in each trial and trials were separated by two or three TRs. These intertrial intervals occurred equally often and were randomly assigned to the object presentations. The presentation of object images was locked to the onset of the new fMRI volume. For each participant, we generated a trial order adhering to the above constraints and used the identical trial order for the picture viewing tasks before and after learning the spatio-temporal arrangement of objects along the route. Using the exact same temporal structure of object presentations in both runs rules out potential effects of temporal autocorrelation of the BOLD signal on the results, since such a spurious influence on the representational structure would be present in both tasks similarly and therefore cannot drive the pattern similarity *change* we focussed our analysis on (Deuker et al., 2016).

MRI Acquisition

All MRI data were collected using a 3T Siemens Skyra scanner (Siemens, Erlangen, Germany). Functional images during the picture viewing tasks were acquired with a 2D EPI sequence (voxel size 1.5mm isotropic, TR=2270ms, TE=24ms, 40 slices, distance factor 13%, flip angle 85°, field of view (FOV) 210×210×68mm). The FOV was oriented to fully cover the medial temporal lobes and if possible calcarine sulcus (Deuker et al., 2016). To improve the registration of the functional images with partial coverage of the brain, 10 volumes of the same functional sequence with an increased number of slices (120 slices, TR=6804.1ms) were acquired (see fMRI

preprocessing). Additionally, gradient field maps were acquired (for 21 participants) with a gradient echo sequence (TR=1020 ms; TE1=10ms; TE2=12.46ms; flip angle=90˚; volume resolution=3.5×3.5×2mm; FOV = 224×224 mm). Further, a structural image was acquired for each participant (voxel size = 0.8×0.8×0.8mm, TR=2300ms; TE=315ms; flip angle=8˚; in-plane resolution=256×256 mm; 224 slices).

Quantification and statistical analysis

Behavioral Data

Results from in-depth analysis of the behavioral data obtained during the spatio-temporal learning task as well as the memory tests conducted after fMRI scanning are reported in detail in (Deuker et al., 2016). Here, we used data from the spatio-temporal learning task as predictions for multi-voxel pattern similarity (see below). Specifically, we defined the temporal structure of pairwise relationships between objects pairs as the median time elapsed between object encounters across the 14 laps of the route. These times differed between participants due to differences in navigation speed (Deuker et al., 2016). Figure 1b shows the temporal distance matrix averaged across participants for illustration. The spatial distances between object positions were defined as the Euclidean distances between the locations of the respective chests in the virtual city. For details of the analysis quantifying the relationship between entorhinal pattern similarity change and recall behavior see the corresponding section below.

fMRI preprocessing

Preprocessing of FMRI data was carried out using FEAT (FMRI Expert Analysis Tool, version 6.00), part of FSL (FMRIB's Software Library, www.fmrib.ox.ac.uk/fsl, version 5.0.8), as described in (Deuker et al., 2016). Functional images were submitted to motion correction and high-pass filtering (cutoff 100s). Images were not smoothed. When available, distortion correction using the fieldmaps was applied. Using FLIRT (Jenkinson and Smith, 2001; Jenkinson et al., 2002), the functional images acquired during the picture viewing tasks were registered to the preprocessed whole-brain mean functional images, which were in turn registered to the to the participant's structural scan. The linear registration from this high-resolution structural to standard MNI space (1mm resolution) was then further refined using FNIRT nonlinear registration (Anderson et al., 2010). Representational similarity analysis of the functional images acquired during the picture viewing tasks was carried out in regions of interests co-registered to the space of the whole-brain functional images.

ROI definition

Based on functional connectivity patterns, the anterior-lateral and posterior-medial portions of human EC were identified as human homologue regions of the rodent lateral and medial EC in two independent studies (Navarro Schröder et al., 2015; Maass et al., 2015). Here, we focused on temporal coding in the alEC, building upon a recent report of temporal signals in rodent lateral EC during navigation (Tsao et al., 2018). Therefore, we used masks from (Navarro Schröder et al., 2015) to perform ROI-based representational similarity analysis on our data. For each ROI, the

mask was co-registered from standard MNI space (1mm) to each participant's functional space (number of voxels: alEC 126.7±46.3; pmEC 69.0±32.9). To improve anatomical precision for the EC masks, the subregion masks from (Navarro Schröder et al., 2015) were each intersected with participant-specific EC masks obtained from their structural scan using the automated segmentation implemented in Freesurfer (version 5.3). ROI masks for the bilateral lateral occipital cortex were defined based on the Freesurfer segmentation and intersected with the combined brain masks from the two fMRI runs since this ROI was located at the edge of our field of view.

Representational Similarity Analysis

As described in (Deuker et al., 2016), we implemented representational similarity analysis (RSA, (Kriegeskorte et al., 2008b, 2008a)) for the two picture viewing tasks individually and then analyzed changes in pattern similarity between the two picture viewing tasks, which were separated by the spatio-temporal learning phase. After preprocessing, analyses were conducted in Matlab (version 2017b, MathWorks). In a general linear model, we used the motion parameters obtained during preprocessing as predictors for the time series of each voxel in the respective ROI. Only the residuals of this GLM, i.e. the part of the data that could not be explained by head motion, were used for further analysis. Stimulus presentations during the picture viewing tasks were locked to the onset of fMRI volumes and the third volume after the onset of picture presentations, corresponding to the time 4.54 to 6.81 seconds after stimulus onset, was extracted for RSA.

For each ROI, we calculated Pearson correlation coefficients between all object presentations except for comparisons within the same of the 12 blocks of each picture viewing task. For each pairwise comparison, we averaged the resulting correlation coefficients across comparisons, yielding a 16×16 matrix reflecting the average representational similarity of objects for each picture viewing task (Deuker et al., 2016). These matrices were Fisher z-transformed. Since the picture viewing task was conducted before and after spatio-temporal learning, the two cross-correlation matrices reflected representational similarity with and without knowledge of the spatial and temporal relationships between objects, respectively. Thus, the difference between the two matrices corresponds to the change in pattern similarity due to learning. Specifically, we subtracted the pattern similarity matrix obtained prior to learning from the pattern similarity matrix obtained after learning, resulting in a matrix of pattern similarity change for each ROI from each participant. This change in similarity of object representations was then compared to different predictions of how this effect of learning might be explained (Figure 1B).

To test the hypothesis that multi-voxel pattern similarity change reflects the temporal structure of the object encounters along the route, we correlated pattern similarity change with the temporal relationships between object pairs; defined by the participant-specific median time elapsed between object encounters while navigating the route. Likewise, we compared pattern similarity change to the Euclidean distances between object positions in the virtual city as well as the temporal relations subjectively remembered by each participant. We calculated Spearman correlation coefficients to quantify the fit between pattern similarity change and each prediction. We expected negative correlations as relative increases in pattern similarity are expected for

objects separated by only a small distance compared to comparisons of objects separated by large distances (Deuker et al., 2016). We compared these correlation coefficients to a surrogate distribution obtained from shuffling pattern similarity change against the respective prediction. For each of 10000 shuffles, the Spearman correlation coefficient between the two variables was calculated, yielding a surrogate distribution of correlation coefficients (Figure 1B). We quantified the size of the original correlation coefficient in comparison to the surrogate distribution. Specifically, we assessed the proportion of larger or equal correlation coefficients in the surrogate distribution and converted the resulting p-value into a z-statistic using the inverse of the normal cumulative distribution function (Deuker et al., 2016; Stelzer et al., 2013; Schlichting et al., 2015). Thus, for each participant, we obtained a z-statistic reflecting the fit of the prediction to pattern similarity change in that ROI. For visualization (Figure 2c), we averaged correlation coefficients quantifying pattern similarity change in alEC separately for comparisons of objects encountered close together or far apart in time based on the median elapsed time between object pairs.

The z-statistics were tested on the group level using permutation-based procedures (10000 permutations) implemented in the Resampling Statistical Toolkit for Matlab (https://mathworks.com/matlabcentral/fileexchange/27960-resampling-statistical-toolkit). To test whether pattern similarity change in alEC reflected the temporal structure of object encounters, we tested the respective z-statistic against 0 using a permutation-based t-test and compared the resulting p-value against an alpha of 0.0125 (Bonferroni-corrected for 4 comparisons, Figure 2). Respecting within-subject dependencies, differences between the fit of temporal and spatial relationships between objects and pattern similarity change in the EC subregions were assessed using a permutation-based two-way repeated measures ANOVA with the factors EC subregion (alEC vs. pmEC) and relationship type (elapsed time vs. Euclidean distance). Planned post-hoc comparisons then included permutation-based t-tests of temporal against spatial mapping in alEC and temporal mapping between alEC and pmEC (Bonferroni-corrected alpha-level of 0.025).

Accounting for adjacency effects

To account for the effects of temporal adjacency we applied a two-step procedure. In a first step, we used a GLM for each participant to test the effect of temporal adjacency using a binary predictor (ones for temporally adjacent object pairs, zeros for all other pairs). The resulting t-values were tested against 0 to assess pattern similarity changes of adjacent object pairs across our sample. In a second step, we tested whether pattern similarity change in alEC reflected temporal relationships above and beyond the effects of temporal adjacency. Specifically, we repeated the original analysis on the residuals of the GLMs from the first step, i.e. we assessed correlations between elapsed time and pattern similarity change that could not be explained by increased similarity for adjacent object pairs (Figure S3A, one-sided permutation-based t-test against 0). The z-values of this analysis were used for the correlation with recall behavior described below and shown in Figure 2D.

Relationship of pattern similarity change and recall behavior

We assessed participants' tendency to reproduce objects encountered closely in time along the route at nearby positions during free recall. In this task, conducted after the post-learning picture viewing task, participants had two minutes to name as many of the objects encountered in the virtual city as possible and to speak the names in the order in which they came to mind into a microphone (Deuker et al., 2016). For each pair of recalled objects we calculated the absolute positional difference in reproduction order and correlated these recall distances with elapsed time between object encounters of these pairs. This resulted in high Pearson correlation coefficients for participants with the tendency to recall objects at distant temporal positions along the route far apart and to retrieve objects encountered closely together in time along the route at nearby positions during memory retrieval. Such a temporally structured recall order would result for example from mentally traversing the route during the free recall task. The temporal structure of participants' free recall was significantly correlated with the strength of the relationship between elapsed time and pattern similarity change not explained by the adjacency model (Figure 2D). This Pearson correlation was also significant when excluding one participant identified as a bivariate outlier ($r=-0.53$, $p=0.007$, CIs: -0.76, -0.17) using the Robust Correlation Toolbox (Pernet et al., 2013).

Temporal intervals during the baseline scan

We interpret pattern similarity change between the picture viewing tasks as being induced by the learning task. To rule out effects of temporal intervals between objects experienced outside of the virtual city we correlated pattern similarity change in the alEC with temporal relationships during the pre-learning baseline scan. Specifically, we calculated the average temporal distance during the first picture viewing task for each pair of objects. Analogous to the time elapsed during the task, we correlated these temporal distances with pattern similarity change in the alEC. One participant was excluded from this analysis due to a z-value more than 1.5 times the interquartile range below the lower quartile. We tested whether pattern similarity change differed from zero and whether correlations with elapsed time during the task were more negative than correlations with temporal distance during the first picture viewing task (one-sided test) using permutation-based t-tests (Figure S3B).

Timeline reconstruction

To reconstruct the timeline of events from alEC pattern similarity change we combined multidimensional scaling with Procrustes analysis (Figure 2A). We first rescaled the pattern similarity matrix to a range from 0 to 1 and then converted it to a distance matrix (distance = 1-similarity). We averaged the distance matrices across participants and subjected the resulting matrix to classical multidimensional scaling. Since we were aiming to recover the timeline of events, we extracted coordinates underlying the averaged pattern distance matrix along one dimension. In a next step, we fitted the resulting coordinates to the times of object encounters along the route, which were also averaged across participants, using Procrustes analysis. This analysis finds the linear transformation, allowing scaling and reflections, that minimizes the sum

of squared errors between the two sets of temporal coordinates. To assess whether the reconstruction of the temporal relationships between memories was above chance, we correlated the reconstructed temporal coordinates with the true temporal coordinates using Pearson correlation (Figure 2B). 95% confidence intervals were bootstrapped using the Robust Correlation Toolbox (Pernet et al., 2013). Additionally, we compared the goodness of fit of the Procrustes transform—the Procrustes distance, which measures the deviance between true and reconstructed coordinates—to a surrogate distribution. Specifically, we randomly shuffled the true temporal coordinates and then mapped the coordinates from multidimensional scaling onto these shuffled timelines. We computed the Procrustes distance for each of 10000 iterations. We quantified the proportion of random fits in the surrogate distribution better than the fit to the true timeline (i.e. smaller Procrustes distances) and expressed it as a p-value to demonstrate that our reconstruction exceeds chance level (Figure 2C-D).

Signal-to-noise ratio

We quantified the temporal and spatial signal-to-noise ratio for each ROI. Temporal signal-to-noise was calculated for each voxel as the temporal mean divided by the temporal standard deviation for both runs of the picture viewing task separately. Values were averaged across the two runs and across voxels in the ROIs. Spatial signal-to-noise ratio was calculated for each volume as the mean signal divided by the standard deviation across voxels in the ROI. The resulting values were averaged across volumes of the time series and averaged across the two runs. Signal-to-noise ratios were compared between ROIs using permutation-based t-tests.

Supplemental Figures

Figure S1

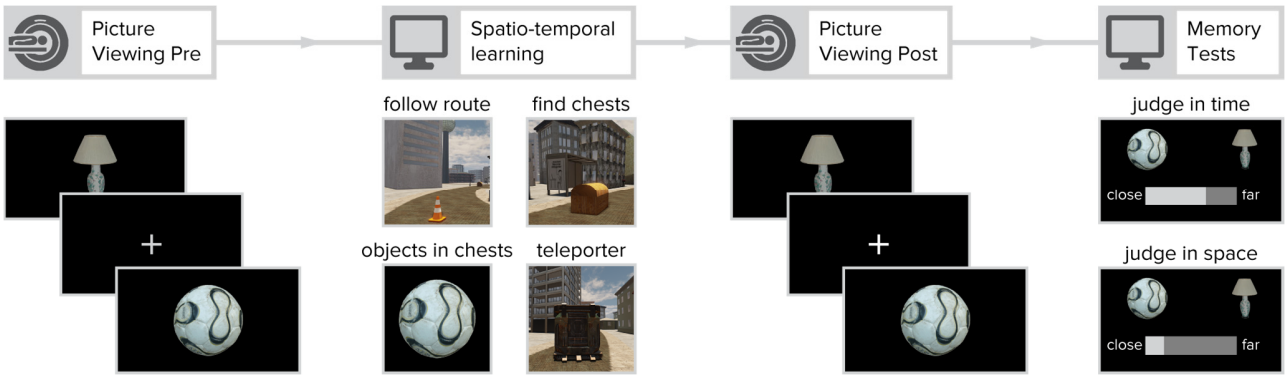

Figure S1. Related to Figure 1. Overview of experimental design. Participants viewed object images in random order while undergoing fMRI before and after learning the temporal and spatial relationships between these objects. The order and timing of picture presentations was held identical in both sessions to assess changes in the similarity of object representations as measured by the difference in similarity of multi-voxel activity patterns (see Methods). In between the two picture viewing tasks, participants acquired knowledge about the spatial and temporal positions of objects along a route through the virtual city. Initially, the route was marked by traffic cones, but in later laps participants navigated the route without guidance. Participants encountered chests along the route and were instructed to open the chests by walking into them. Each chest contained a different object, which was displayed on a black screen upon opening the chest. Crucially, the route featured three teleporters that instantly teleported participants to a different part of the city where the route continued (Figure 1). This manipulation enabled us to dissociate the temporal and spatial distances between pairwise object comparisons (Figure S2). After the second picture viewing task, participants' memory for temporal and spatial relationships between object pairs was assessed. Here, participants adjusted a slider to indicate whether they remembered object pairs to be close together or far apart. Temporal and spatial relations were judged in separate trials. The results of these memory tests are reported in detail in (Deuker et al., 2016).

Figure S2

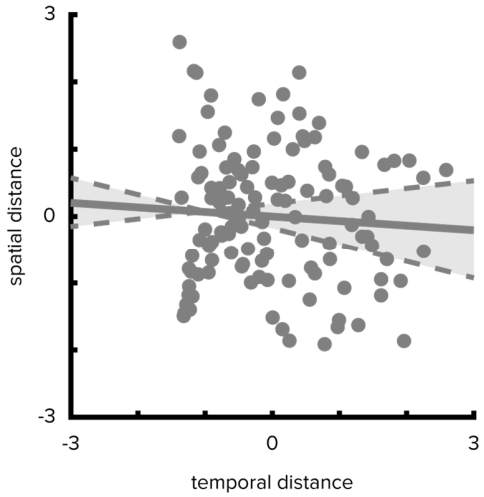

Figure S2. Related to Figures 1 and 2. Temporal and spatial distances are uncorrelated. Pairwise temporal and spatial distances between objects are uncorrelated (Pearson r=-0.068; bootstrapped 95% confidence interval: -0.24, 0.12; p=0.462). Median times elapsed between object encounters were z-scored and then averaged across participants. Spatial distances were defined as z-scored Euclidean distances between object positions. When correlating individual median times elapsed with spatial distances, the correlation between the dimensions was not significant in any of the participants (mean ± standard deviation of Pearson correlation coefficients r= -0.068±0.006, all p≥0.378).

Figure S3

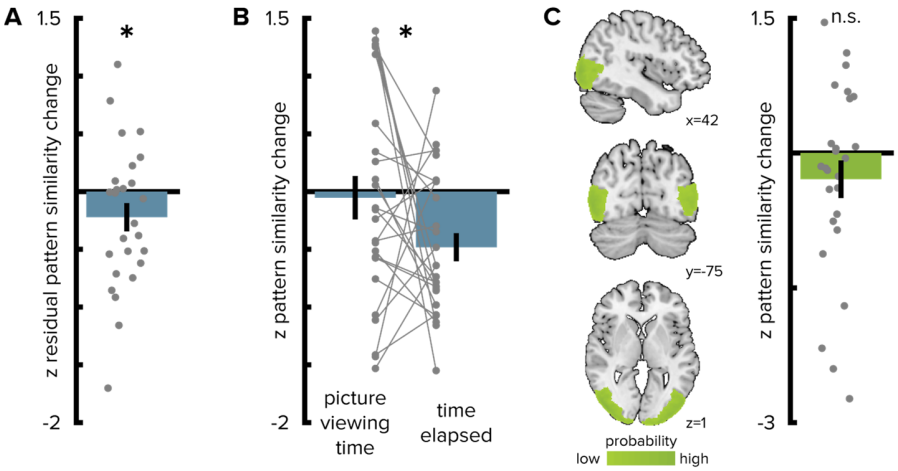

Figure S3. Related to Figure 2. Control analyses. A. We controlled for increased pattern similarity for objects at temporally adjacent positions along the route using a GLM (see Methods). Residuals of this GLM, i.e. pattern similarity that could not be explained by adjacency, were negatively correlated with the time elapsed between object encounters, providing evidence for holistic representations of temporal relationships in alEC. **B.** Pattern similarity change in alEC was not correlated with temporal distances from the first picture viewing task. Correlations with pattern similarity change were more negative for elapsed time during the learning task than for presentation times during the first picture viewing task (see Methods). **C.** Left: Group-level visualization of the region of interest used for the lateral occipital cortex. Right: Pattern similarity change in the lateral occipital cortex was not correlated with the time elapsed between object encounters. Bars show mean and S.E.M.

Figure S4

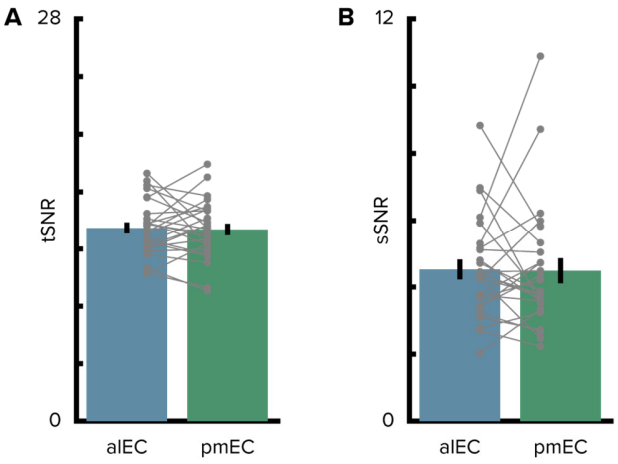

Figure S4. Related to Figure 2. Signal-to-noise ratio in the entorhinal cortex. A. The temporal signal-to-noise ratio did not differ between the entorhinal subregions. **B.** Similarly, the spatial signal-to-noise ratio did not differ between entorhinal subregions. Bars show mean and S.E.M with lines connecting data points from the same participant.

References

Anderson, J., Jenkinson, M., and Smith, S. (2010). Non-linear registration, aka spatial normalisation. FMRIB Tech. Rep. *TR07JA2*.

Barnett, A.J., O'Neil, E.B., Watson, H.C., and Lee, A.C.H. (2014). The human hippocampus is sensitive to the durations of events and intervals within a sequence. Neuropsychologia *64*, 1–12.

Bellmund, J.L.S., Deuker, L., and Doeller, C.F. (2018). Donderstown. Open Sci. Framew.

Copara, M.S., Hassan, A.S., Kyle, C.T., Libby, L.A., Ranganath, C., and Ekstrom, A.D. (2014). Complementary Roles of Human Hippocampal Subregions during Retrieval of Spatiotemporal Context. J. Neurosci. *34*, 6834–6842.

Davachi, L., and DuBrow, S. (2015). How the hippocampus preserves order: the role of prediction and context. Trends Cogn. Sci. *19*, 92–99.

Deuker, L., Bellmund, J.L.S., Navarro Schröder, T., and Doeller, C.F. (2016). An event map of memory space in the hippocampus. ELife *5*, e16534.

DuBrow, S., and Davachi, L. (2014). Temporal Memory Is Shaped by Encoding Stability and Intervening Item Reactivation. J. Neurosci. *34*, 13998–14005.

DuBrow, S., and Davachi, L. (2016). Temporal binding within and across events. Neurobiol. Learn. Mem. *134*, 107–114.

Eichenbaum, H. (2014). Time cells in the hippocampus: a new dimension for mapping memories. Nat. Rev. Neurosci. *15*, 732–744.

Ezzyat, Y., and Davachi, L. (2014). Similarity Breeds Proximity: Pattern Similarity within and across Contexts Is Related to Later Mnemonic Judgments of Temporal Proximity. Neuron *81*, 1179–1189.

Folkerts, S., Rutishauser, U., and Howard, M.W. (2018). Human episodic memory retrieval is accompanied by a neural contiguity effect. J. Neurosci. 2312–2317.

Garvert, M.M., Dolan, R.J., and Behrens, T.E. (2017). A map of abstract relational knowledge in the human hippocampal–entorhinal cortex. ELife *6*, e17086.

Heys, J.G., and Dombeck, D.A. (2018). Evidence for a subcircuit in medial entorhinal cortex representing elapsed time during immobility. Nat. Neurosci. *21*, 1574.

Howard, M.W. (2018). Memory as Perception of the Past: Compressed Time in Mind and Brain. Trends Cogn. Sci. *22*, 124–136.

Howard, M.W., and Kahana, M.J. (2002). A Distributed Representation of Temporal Context. J. Math. Psychol. *46*, 269–299.

Howard, M.W., Fotedar, M.S., Datey, A.V., and Hasselmo, M.E. (2005). The Temporal Context Model in Spatial Navigation and Relational Learning: Toward a Common Explanation of Medial Temporal Lobe Function Across Domains. Psychol. Rev. *112*, 75–116.

Hsieh, L.-T., Gruber, M.J., Jenkins, L.J., and Ranganath, C. (2014). Hippocampal Activity Patterns Carry Information about Objects in Temporal Context. Neuron *81*, 1165–1178.

Jenkins, L.J., and Ranganath, C. (2010). Prefrontal and Medial Temporal Lobe Activity at Encoding Predicts Temporal Context Memory. J. Neurosci. *30*, 15558–15565.

Jenkins, L.J., and Ranganath, C. (2016). Distinct neural mechanisms for remembering when an event occurred. Hippocampus *26*, 554–559.

Jenkinson, M., and Smith, S. (2001). A global optimisation method for robust affine registration of brain images. Med. Image Anal. *5*, 143–156.

Jenkinson, M., Bannister, P., Brady, M., and Smith, S. (2002). Improved Optimization for the Robust and Accurate Linear Registration and Motion Correction of Brain Images. NeuroImage *17*, 825–841.

Kraus, B.J., Brandon, M.P., Robinson, R.J., Connerney, M.A., Hasselmo, M.E., and Eichenbaum, H. (2015). During Running in Place, Grid Cells Integrate Elapsed Time and Distance Run. Neuron *88*, 578–589.

Kriegeskorte, N., Mur, M., and Bandettini, P. (2008a). Representational similarity analysis - connecting the branches of systems neuroscience. Front. Syst. Neurosci. *2*, 4–4.

Kriegeskorte, N., Mur, M., Ruff, D.A., Kiani, R., Bodurka, J., Esteky, H., Tanaka, K., and Bandettini, P.A. (2008b). Matching Categorical Object Representations in Inferior Temporal Cortex of Man and Monkey. Neuron *60*, 1126–1141.

Kumaran, D., and Maguire, E.A. (2006). An Unexpected Sequence of Events: Mismatch Detection in the Human Hippocampus. PLOS Biol. *4*, e424.

Kyle, C.T., Smuda, D.N., Hassan, A.S., and Ekstrom, A.D. (2015). Roles of human hippocampal subfields in retrieval of spatial and temporal context. Behav. Brain Res. *278*, 549–558.

Lositsky, O., Chen, J., Toker, D., Honey, C.J., Shvartsman, M., Poppenk, J.L., Hasson, U., and Norman, K.A. (2016). Neural pattern change during encoding of a narrative predicts retrospective duration estimates. ELife *5*, e16070.

Maass, A., Berron, D., Libby, L., Ranganath, C., and Düzel, E. (2015). Functional subregions of the human entorhinal cortex. ELife *4*, e06426.

MacDonald, C.J., Lepage, K.Q., Eden, U.T., and Eichenbaum, H. (2011). Hippocampal "Time Cells" Bridge the Gap in Memory for Discontiguous Events. Neuron *71*, 737–749.

Mau, W., Sullivan, D.W., Kinsky, N.R., Hasselmo, M.E., Howard, M.W., and Eichenbaum, H. (2018). The Same Hippocampal CA1 Population Simultaneously Codes Temporal Information over Multiple Timescales. Curr. Biol. *28*, 1499-1508.e4.

Milivojevic, B., Vicente-Grabovetsky, A., and Doeller, C.F. (2015). Insight Reconfigures Hippocampal-Prefrontal Memories. Curr. Biol. *25*, 821–830.

Navarro Schröder, T., Haak, K.V., Zaragoza Jimenez, N.I., Beckmann, C.F., and Doeller, C.F. (2015). Functional topography of the human entorhinal cortex. ELife *4*, e06738.

Nielson, D.M., Smith, T.A., Sreekumar, V., Dennis, S., and Sederberg, P.B. (2015). Human hippocampus represents space and time during retrieval of real-world memories. Proc. Natl. Acad. Sci. *112*, 11078–11083.

Pastalkova, E., Itskov, V., Amarasingham, A., and Buzsáki, G. (2008). Internally Generated Cell Assembly Sequences in the Rat Hippocampus. Science *321*, 1322–1327.

Pernet, C.R., Wilcox, R.R., and Rousselet, G.A. (2013). Robust Correlation Analyses: False Positive and Power Validation Using a New Open Source Matlab Toolbox. Front. Psychol. *3*.

Ranganath, C. (2018). Time, memory, and the legacy of Howard Eichenbaum. Hippocampus 1–16.

Ranganath, C., and Ritchey, M. (2012). Two cortical systems for memory-guided behaviour. Nat. Rev. Neurosci. *13*, 713–726.

Ritchey, M., Libby, L.A., and Ranganath, C. (2015). Cortico-hippocampal systems involved in memory and cognition: the PMAT framework. In Progress in Brain Research, (Elsevier), pp. 45–64.

Schapiro, A.C., Kustner, L.V., and Turk-Browne, N.B. (2012). Shaping of object representations in the human medial temporal lobe based on temporal regularities. Curr. Biol. CB *22*, 1622–1627.

Schapiro, A.C., Turk-Browne, N.B., Norman, K.A., and Botvinick, M.M. (2016). Statistical learning of temporal community structure in the hippocampus. Hippocampus *26*, 3–8.

Schlichting, M.L., Mumford, J.A., and Preston, A.R. (2015). Learning-related representational changes reveal dissociable integration and separation signatures in the hippocampus and prefrontal cortex. Nat. Commun. *6*.

Stelzer, J., Chen, Y., and Turner, R. (2013). Statistical inference and multiple testing correction in classification-based multi-voxel pattern analysis (MVPA): Random permutations and cluster size control. NeuroImage *65*, 69–82.

Thavabalasingam, S., O'Neil, E.B., and Lee, A.C.H. (2018). Multivoxel pattern similarity suggests the integration of temporal duration in hippocampal event sequence representations. NeuroImage *178*, 136–146.

Tsao, A., Sugar, J., Lu, L., Wang, C., Knierim, J.J., Moser, M.-B., and Moser, E.I. (2018). Integrating time from experience in the lateral entorhinal cortex. Nature *561*, 57–62.

Tubridy, S., and Davachi, L. (2011). Medial Temporal Lobe Contributions to Episodic Sequence Encoding. Cereb. Cortex *21*, 272–280.

Wang, F., and Diana, R.A. (2017). Temporal context in human fMRI. Curr. Opin. Behav. Sci. *17*, 57–64.

Acknowledgments

The authors would like to thank Raphael Kaplan for comments on a previous version of this manuscript. C.F.D.'s research is supported by the Max Planck Society; the European Research Council (ERCCoG GEOCOG 724836); the Kavli Foundation, the Centre of Excellence scheme of the Research Council of Norway – Centre for Neural Computation, The Egil and Pauline Braathen and Fred Kavli Centre for Cortical Microcircuits, the National Infrastructure scheme of the Research Council of Norway – NORBRAIN; and the Netherlands Organisation for Scientific Research (NWO-Vidi 452-12-009; NWO-Gravitation 024-001-006; NWO-MaGW 406-14-114; NWO-MaGW 406-15-291). The funders had no role in study design, data collection and analysis, decision to publish or preparation of the manuscript.

Author Contributions

L.D., C.F.D. and J.L.S.B. conceived and designed the experiment. L.D. and J.L.S.B. collected the data. J.L.S.B. and L.D. analyzed the data. J.L.S.B. wrote the manuscript, with input from L.D. and C.F.D. All authors discussed the results and contributed to the final manuscript.

Competing Financial Interests Statement

The authors declare no competing financial interests.